Supporting Information

A Multi-Stage COF Membrane Column System for Enhanced Yb/Lu Separation

Yingdan Zhang, ‡ Pan He, ‡ Yingdi Zou, Xiaomeng Huang, Jie Zhang, Zhiying Fan, Ningning He, Yang Li*, and Lijian Ma*

College of Chemistry, Sichuan University, Key Laboratory of Radiation Physics & Technology, Ministry of Education Chengdu, 610064, China

** Corresponding authors: E-mail: ly7701850@163.com (Y. Li), ma.lj@hotmail.com (L. Ma)*

Table of Contents

Section S1 Material and methods

1.1. Chemicals and materials

The reagents and solvents used in the experiments were as follows: Tris(4-aminophenyl)amine (TAPA) and 1,3,5-triformylphloroglucinol (Tp) were purchased from Aladdin Chemistry Co., Ltd. (China). $Lu(NO_3)_3$, and $Yb(NO_3)_3$ were also obtained from the same supplier. Additionally, N,N-dimethylformamide (DMF), acetic acid, dichloromethane (DCM), ethanol, and methanol were sourced from Chengdu Forest Science & Technology Development Co., Ltd. (China). All reagents and solvents used in the experiments were of commercial grade and were used without further purification.

1.2. Synthetic procedures

1.2.1. Preparation of S-COF powder by emulsion template method

TAPA (0.1 mmol, corresponding to 29 mg) and Tp (0.1 mmol, equivalent to 21 mg) were meticulously weighed into glass bottles, subsequently dissolved, and thoroughly dispersed through the addition of 3 mL of acetone. Under agitation, 0.1 mL of 6 M acetic acid was added, followed by stirring for 30 seconds post-addition. The mixture was then allowed to stand undisturbed at room temperature for a period of 3 days. The resulting precipitate was filtered and exhaustively washed by methanol, ethanol, and DMF. Then, dried at 60 °C under vacuum for 12 hours. The S-COF was red powder.

1.2.2. Preparation of M-COF powder by interface method

The buffer interlayer interface method was used to prepare for M-COF. First, a certain amount of Tp (0.1 mmol, 21 mg) was dissolved in 80 mL CH_2Cl_2 solution, and acetic acid solution (6 M, 30 mL) was slowly added to the top of CH_2Cl_2 solution as a buffer layer and catalyst. TAPA (0.1 mmol, 29 mg) was dissolved in 50 mL DMF solution and acetic acid solution was slowly added to the upper layer. The reaction was allowed to stand for three days at room temperature, the solution was filtered, the intermediate membrane product was collected, and the resulting membrane product was thoroughly cleaned with ethanol, DMF, and methanol. Then, dried at 60 °C under vacuum for 12 hours. The M-COF was orange powder.

1.2.3. Preparation of S-COF@P507 and M-COF@P507

To prepare COF@P507, 300 mg of COF (S-COF or M-COF) sample and 75 mg of P507 were accurately weighed and placed in a round-bottom flask, followed by the addition of 20 mL of anhydrous methanol. The mixture was sonicated for 30 minutes to ensure thorough mixing of the COF material and P507. Subsequently, the methanol was removed using a rotary evaporator, yielding COF@P507 with a 25% mass loading. The product was dried overnight in a vacuum oven at 60°C to completely remove residual methanol and prevent the detachment of P507. Therefore, P507 was physically adsorbed onto the COF matrix. During preliminary optimization experiments, we found that a low loading of P507 resulted in poor separation performance, while a higher loading increased the difficulty of elution and caused severe sample stickiness. Thus, a 25% loading was selected.

1.3. Column separation test investigations

2.60 g $Yb(NO_3)_3 \cdot 5H_2O$ and 2.68 g $Lu(NO_3)_3 \cdot 6H_2O$ were dissolved in 1 L of deionized water to prepare a stock solution of Yb^{3+} and Lu^{3+} at 1000 ppm. The prepared Yb^{3+} and Lu^{3+} stock solutions were diluted to the desired different concentrations. The S-COF@P507 or M-COF@P507 powder was dispersed with deionized water, then loaded into a quartz column (inner diameter = 5.0 mm, length = 100 mm), sealed with fat-free cotton, filled to the desired height, and added fat-free cotton at the top to prevent material dispersion. Negative pressure was applied to the separator column through a peristaltic pump to allow fluid outflow. The liquid was collected in fractions of 1 mL, diluted twice and analyzed for ion concentration by ICP-OES to determine the elution curve.

As an important parameter to evaluate the separation performance, the recovery rate, R is calculated by following equation:

$$R = \frac{C_V \times V}{m_0}$$

where C_v is the ion concentration in the collected components, and m_0 is initial mass of the associated metal ions. V is the volume of the collected solution.

The DF is used to evaluate the column separation performance, and the formula is as follows:

$$DF = \frac{m_{Yb,0}/m_{Lu,0}}{m_{Yb,elute}/m_{Lu,elute}}$$

$m_{Yb,0}$ and $m_{Lu,0}$ for separation of Yb and Lu before initial mass, $m_{Yb,elute}$ and $m_{Lu,elute}$ are the mass of Yb and Lu contained in the collection solution after the intersection of the elution curves.

1.4. Radioactive tracer experiments

0.1 μCi of ^{177}Lu and 1.0 mL of Yb (III) and Lu (III) aqueous solutions at the indicated concentrations were added to 2 mL EP tubes. 1 mL of the above solution was used for separation and another 1 mL was used for attenuation correction. For the collection solution containing ^{177}Lu, the elution curve was determined by NaI (Tl) scintillation detector. After two $t_{1/2}$ (about 14 d), the Yb content was determined by ICP-OES to obtain the final elution curve of Yb.[1]

1.5. Static adsorption

Langmuir equation:

$$\frac{C_e}{q_e} = \frac{1}{q_{max}K_L} + \frac{C_e}{q_{max}}$$

Where K_L (L mg^{-1}) is the Langmuir constant related to the binding site affinity, and q_{max} (mg g^{-1}) is the maximum adsorption capacity. It can be calculated by the fitting curve of C_e/q_e and C_e.[2]

The Freundlich model is used for multi-layer adsorption, and the formula is as follows:

$$\ln q_e = \ln K_F + \frac{1}{n}\ln C_e$$

Where K_F (mg/g (L/mg)$^{1/n}$) and n are Freundlich constants related to adsorption capacity and adsorption strength, respectively, which can be calculated from a linear plot of ln q_e versus ln C_e.[2]

Pseudo-first-order kinetic model:

$$\ln (q_e - q_t) = \ln q_e - k_1 t$$

Pseudo-second-order kinetic model:

$$\frac{t}{q_t} = \frac{1}{kq_e^2} + \frac{1}{q_e}t$$

Where, q_e and q_t (mg/g) are the adsorption amount when equilibrium is reached and the adsorption amount at any time t, respectively, and t (h) is the adsorption time. The kinetic constants of k_1 (1/h) for pseudo-first-order adsorption and k_2 (g/mg/h) for pseudo-second-order adsorption were determined. In addition, $q_{e,exp}$ is the amount of adsorption calculated from the

adsorption experiments based on the mass difference, $q_{e,cal}$ is the amount of adsorption calculated from the kinetic model, and R^2 is the correlation coefficient of the fitted curve.

1.6. Characterization

Powder X-ray diffraction patterns (PXRD) of all samples were collected on Bruker D2 PHASER X-ray diffractometer using Cu Kα radiation. Fourier transform infrared spectroscopy (FT-IR) spectra were measured on FT-IR spectrometer (Nicolet Nexus 670FT-IR and NEXUS 670) between the ranges of 4000 to 500 cm^{-1}. X-ray photoelectron spectroscopy (XPS) data were collected using a Kratos ASAM800 spectrometer. Scanning electron microscope (SEM) images and energy dispersive spectroscopy (EDS) mapping were collected using a JEOL JSM-5900LV instrument. The concentrations of metal ions in experiments were measured by an Optima 8000 ICP-OES.

Section S2 The chemical structure of P507.

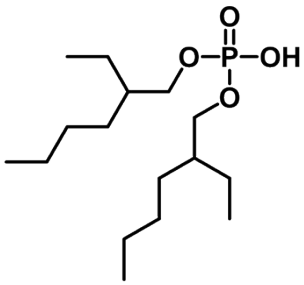

Figure S1 The chemical structure of P507.

Section S3 Characterization of materials

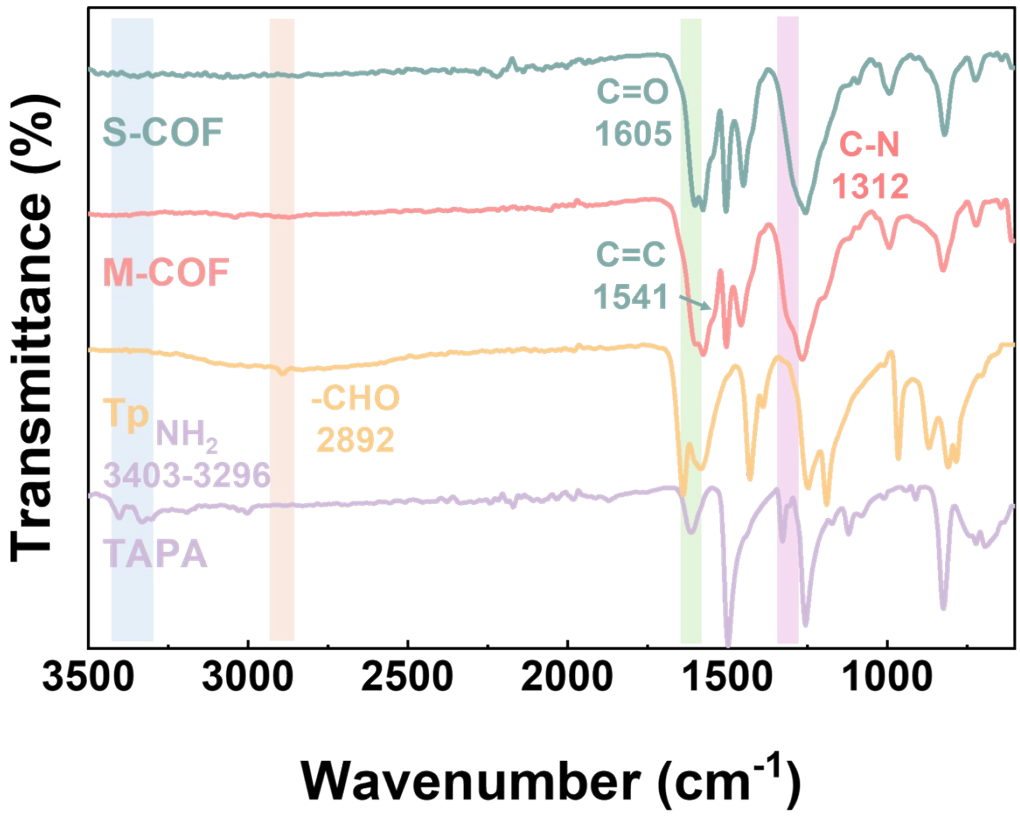

Figure S2 FT-IR spectra of S-COF, M-COF, TAPA, and Tp.

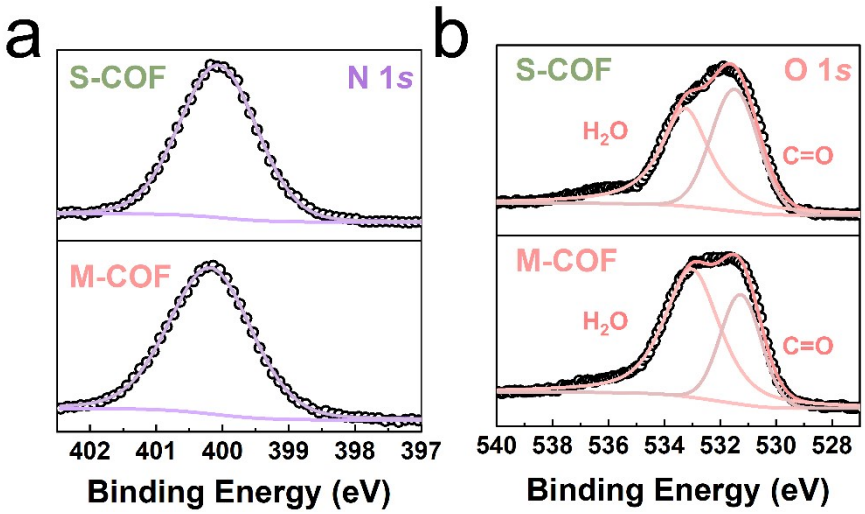

Figure S3 The typical XPS high-resolution spectra of (a) N 1*s*, (b) O 1*s* of S-COF and M-COF.

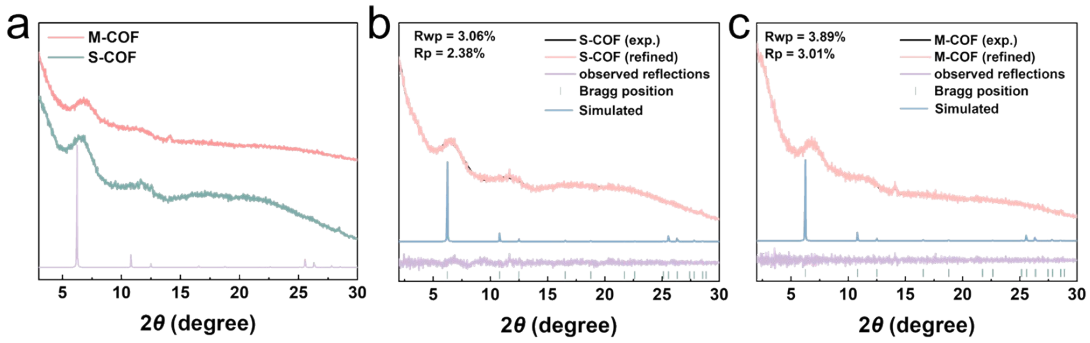

Figure S4 (a) Experimental PXRD patterns of S-COF (green) and M-COF (pink) compared to the simulated AA stacking pattern (purple), (b) Experimental (black) and Pawley-refined (pink) PXRD patterns of S-COF, overlaid with the simulated AA stacking model (blue); observed diffraction peaks (purple) marked below, and (c) Experimental (black) and Pawley-refined (pink) PXRD patterns of M-COF, overlaid with the simulated AA stacking model (blue); observed diffraction peaks (purple) marked below.

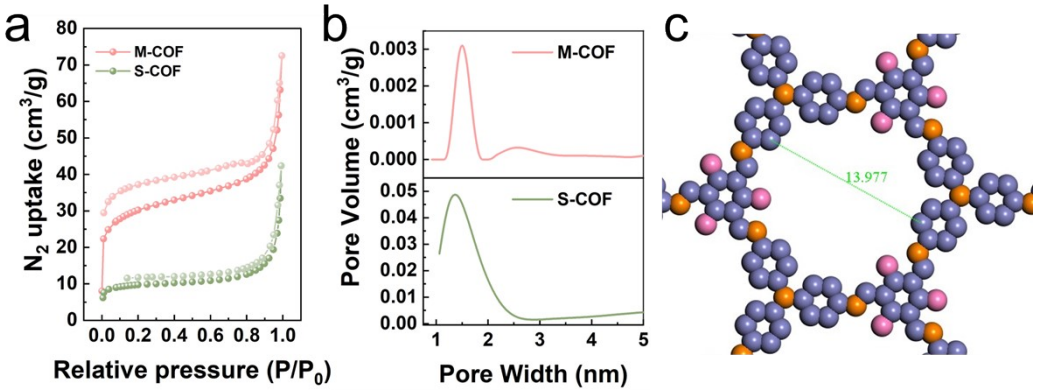

Figure S5 (a) The N_2 adsorption and desorption isotherms of S-COF and M-COF, (b) the pore size distributions of M-COF and S-COF calculated by the NLDFT, and (c) Simulated pore sizes of S-COF and M-COF.

To control the morphology of COF materials, we opted for room-temperature reaction conditions, which however resulted in relatively low crystallinity, and correspondingly low specific surface areas in BET tests. To enhance the specific surface area of S-COF, we increased the activation temperature from 80°C to 120°C. Both materials exhibit non-overlapping adsorption-desorption curves, which we attribute to framework flexibility causing pore contraction during desorption. This phenomenon is supported by: Similar hysteresis has been reported for flexible COFs[3-5], where structural dynamics impede nitrogen release.

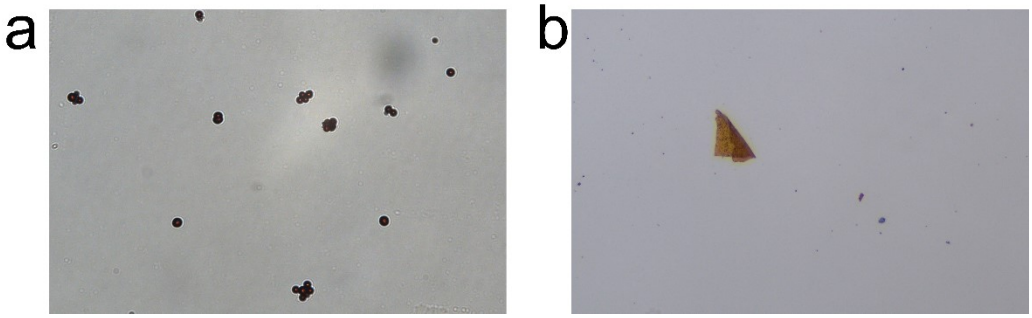

Figure S6 Photographs of (a) S-COF and (b) M-COF under a light microscope (the magnification was 1000).

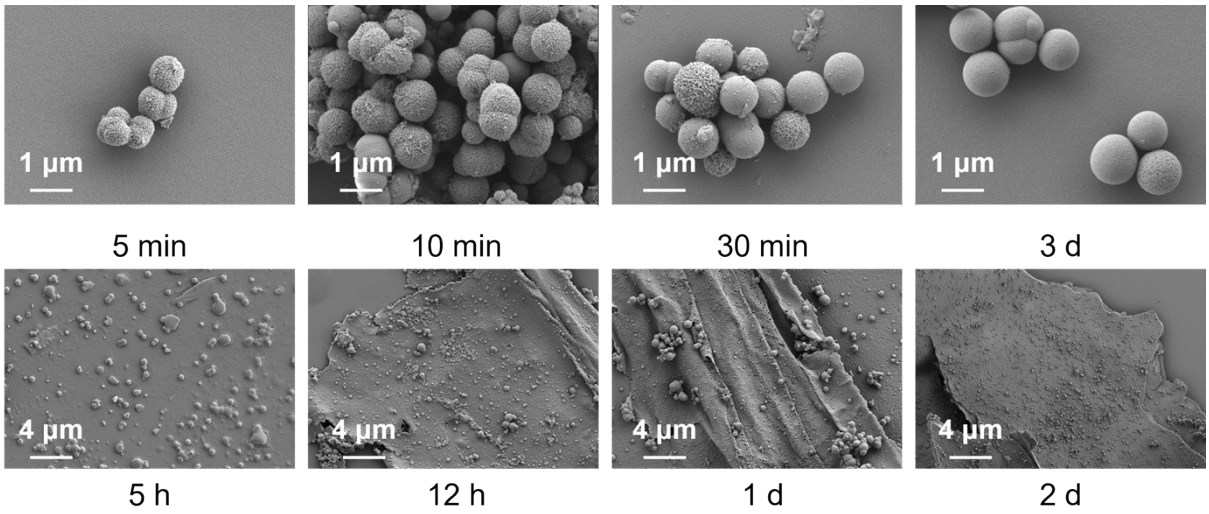

Figure S7 SEM images illustrate the morphological evolution of S-COF and L-COF over time.

As shown in Figure S7, the S-COF within 5 minutes of reaction initiation, spherical nuclei approximately 500 nm in diameter with rough surfaces were observed. These nuclei rapidly grew into micron-sized particles (~1 μm) within 10 minutes while maintaining their rough surface morphology. As the reaction progressed, the particle size stabilized at ~1 μm, and the surface gradually became smoother. In contrast, the interfacial synthesis of M-COF exhibits markedly different kinetics: discrete spherical particles emerged after 5 hours, exhibiting a tendency to assemble into larger aggregates. These particles progressively coalesced, ultimately forming a continuous membrane within 12 hours. Following two days of growth, the membrane developed into a multilayered sheet structure. We hypothesize that the morphological differences between the two methods may arise from their distinct reaction conditions. The solvent method, with its higher reaction concentration, likely promotes faster nucleation and the rapid formation of dispersed spherical particles. In contrast, the interfacial method exhibits constrained molecular diffusion and lower reaction concentration, which favors membrane assembly.

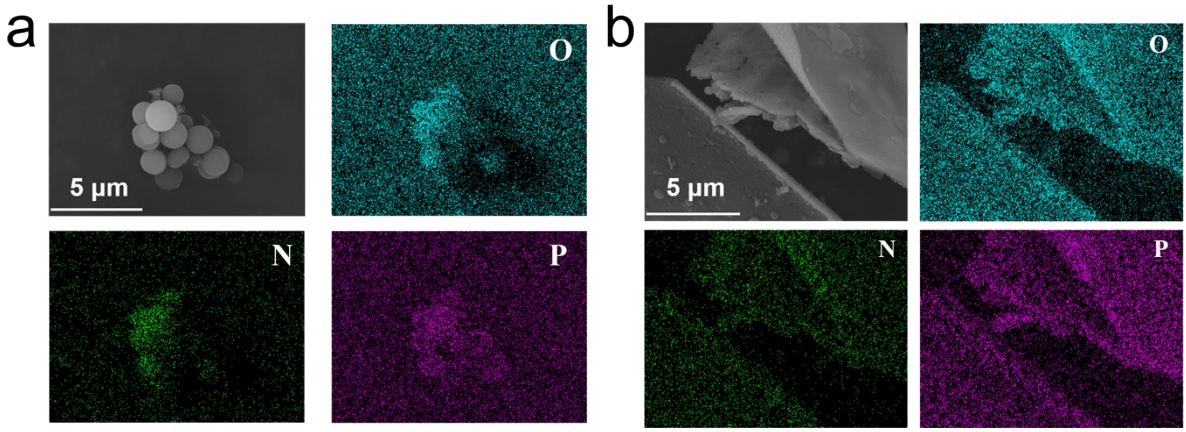

Figure S8 The EDS mapping of (a) S-COF@P507, and (b) M-COF@P507.

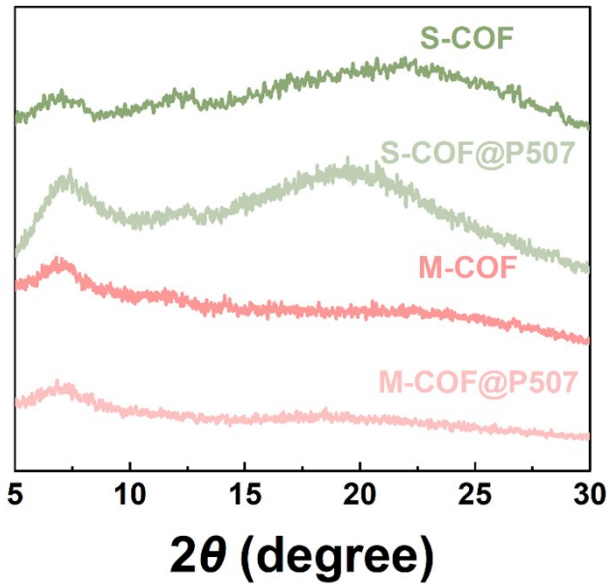

Figure S9 The PXRD patterns of M-COF, S-COF, M-COF@P507, and S-COF@P507.

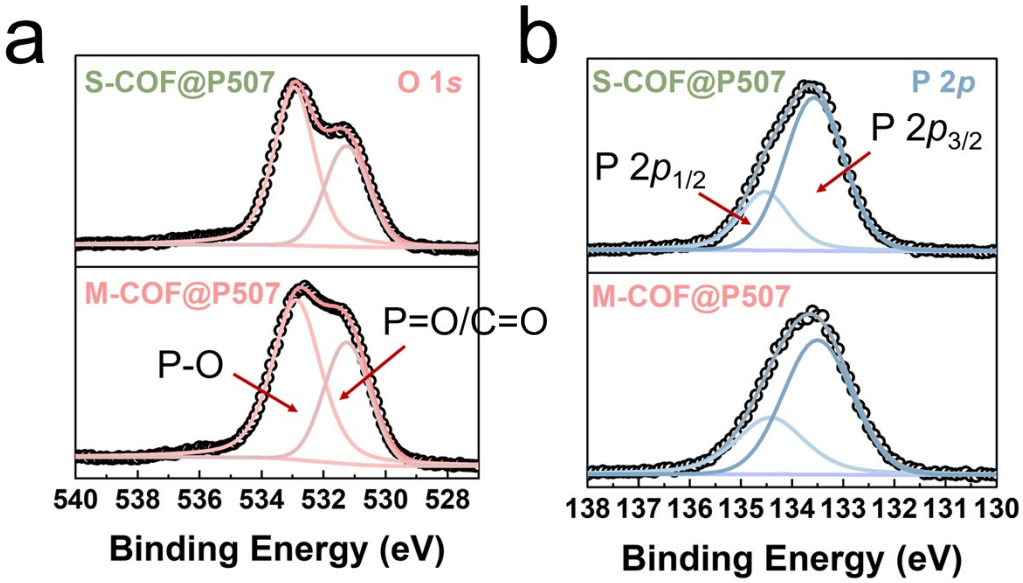

Figure S10 (a) The typical XPS high-resolution spectra of (a) O 1*s*, (b) P 2*p* of S-COF@P507 and M-COF@P507.

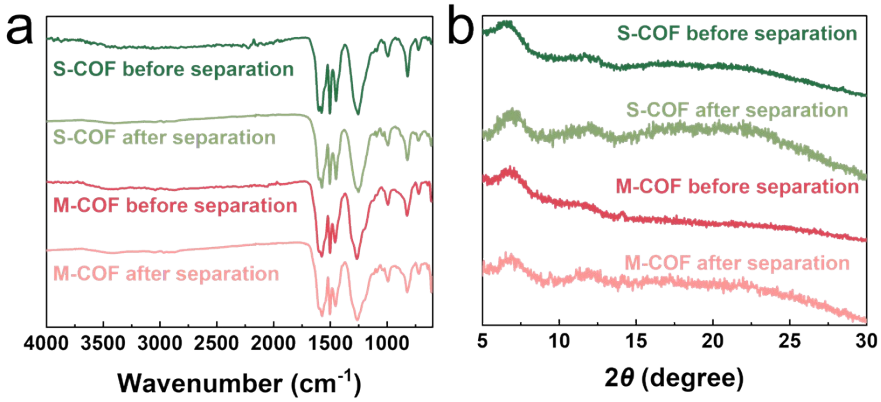

Figure S11 The comparison of (a) FTIR spectra and (b) XRD patterns for S-COF and M-COF materials before and after their application in separation processes.

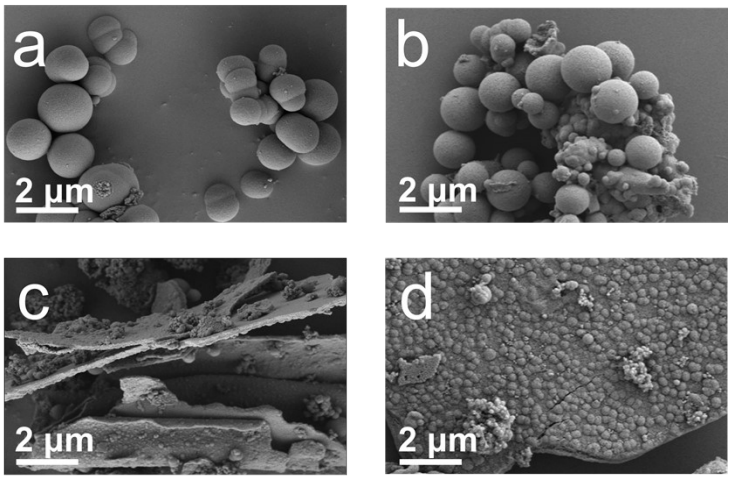

Figure S12 The SEM images of (a) S-COF, (b) S-COF after separation, (c) M-COF, and (d) M-COF after separation.

Section S4 Yb/Lu adsorption

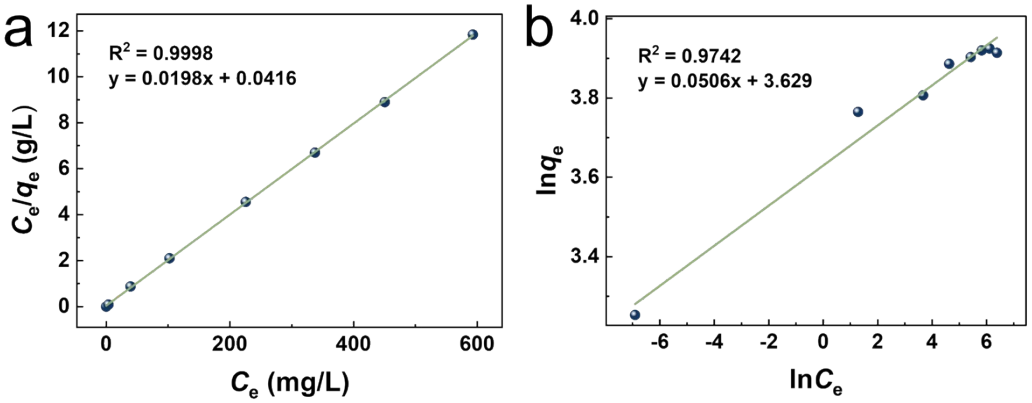

Figure S13 (a) Langmuir isotherm model and (b) Freundlich isotherm model for the sorption of Yb^{3+} onto the M-COF.

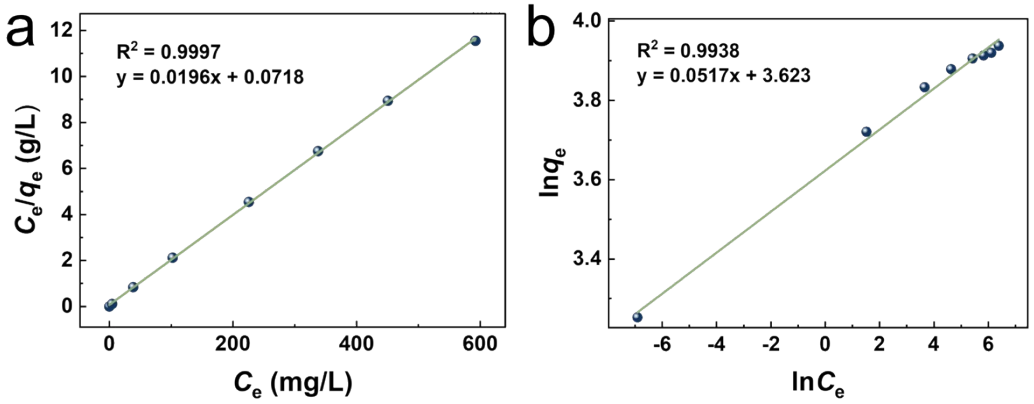

Figure S14 (a) Langmuir isotherm model and (b) Freundlich isotherm model for the sorption of Yb^{3+} onto the S-COF.

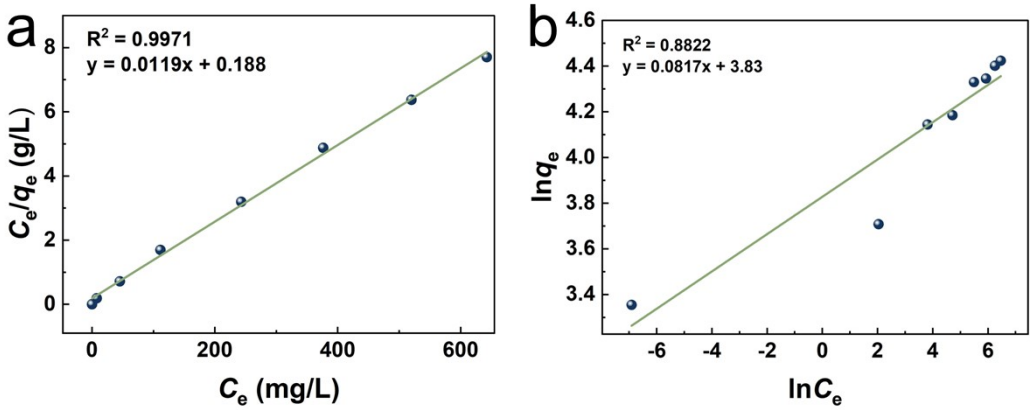

Figure S15 (a) Langmuir isotherm model and (b) Freundlich isotherm model for the sorption of Lu^{3+} onto the M-COF.

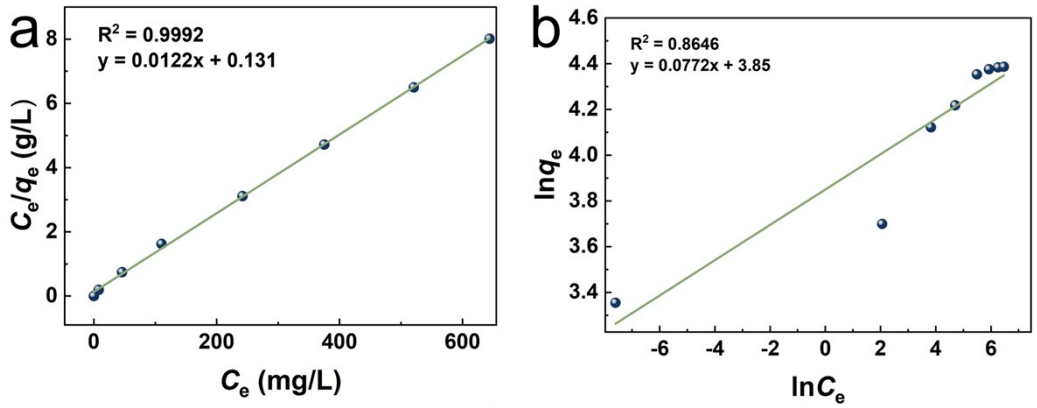

Figure S16 (a) Langmuir isotherm model and (b) Freundlich isotherm model for the sorption of Lu^{3+} onto the S-COF.

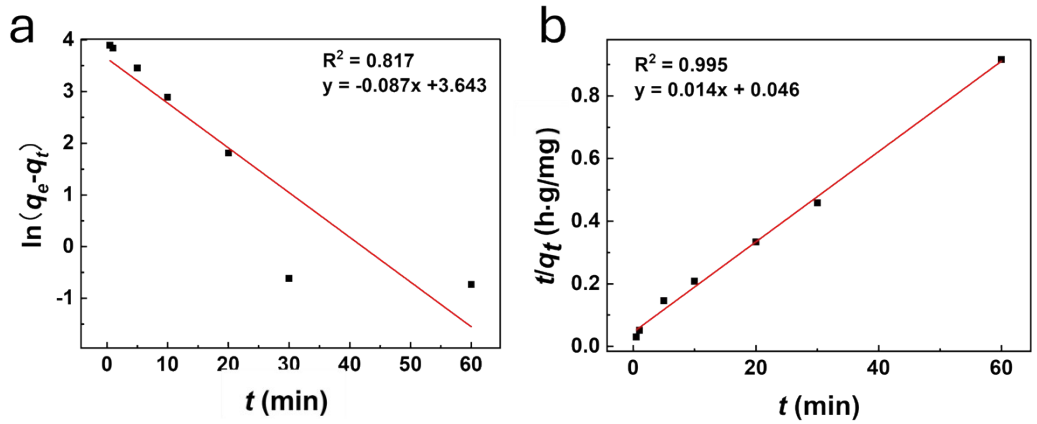

Figure S17 The kinetic model of M-COF for Lu^{3+}: (a) pseudo-first-order model and (b) pseudo-second-order model.

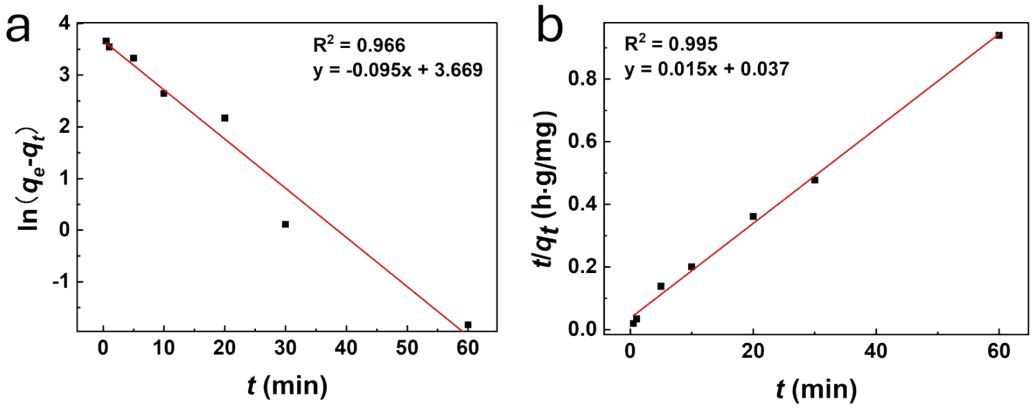

Figure S18 The kinetic model of S-COF for Lu^{3+}: (a) pseudo-first-order model and (b) pseudo-second-order model.

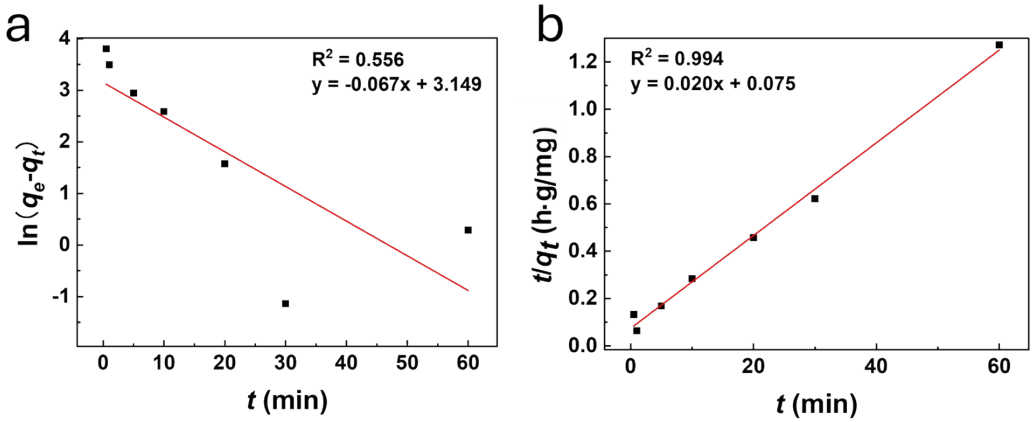

Figure S19 The kinetic model of M-COF for Yb^{3+}: (a) pseudo-first-order model and (b) pseudo-second-order model.

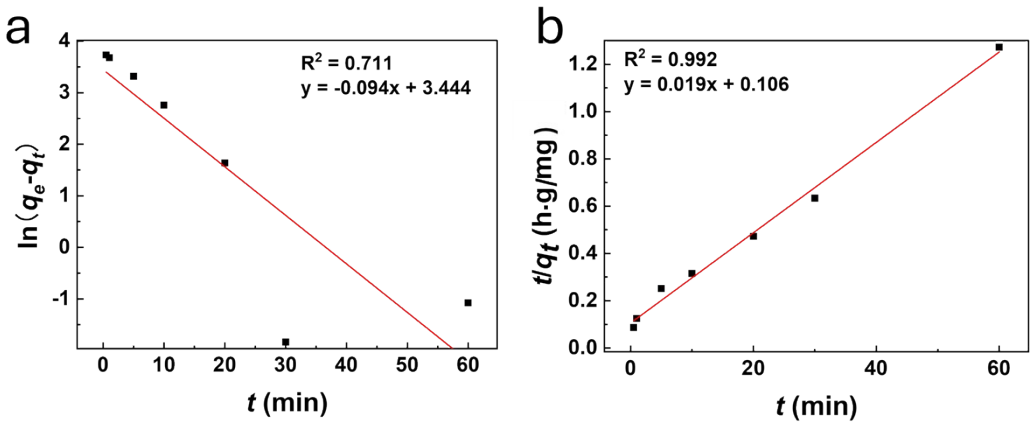

Figure S20 The kinetic model of S-COF for Yb^{3+}: (a) pseudo-first-order model and (b) pseudo-second-order model.

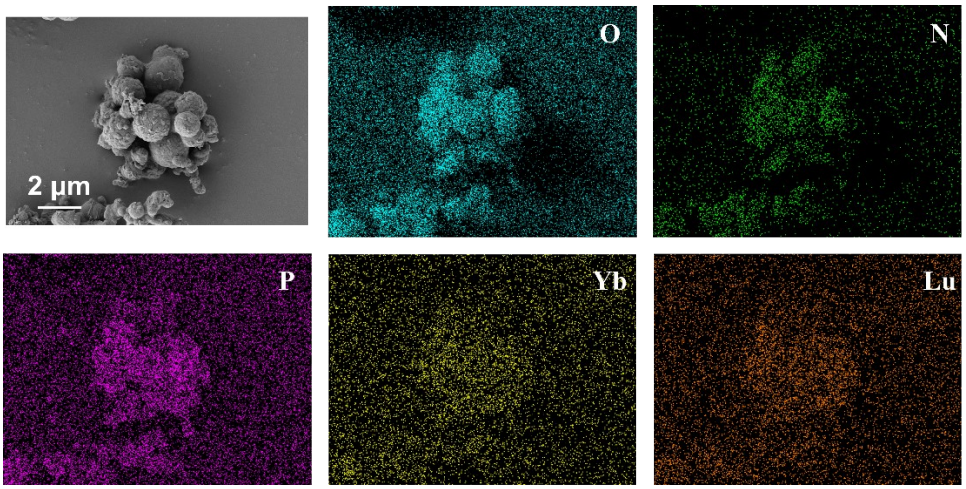

Figure S21 The EDS mapping of S-COF@P507 after adsorption Yb/Lu.

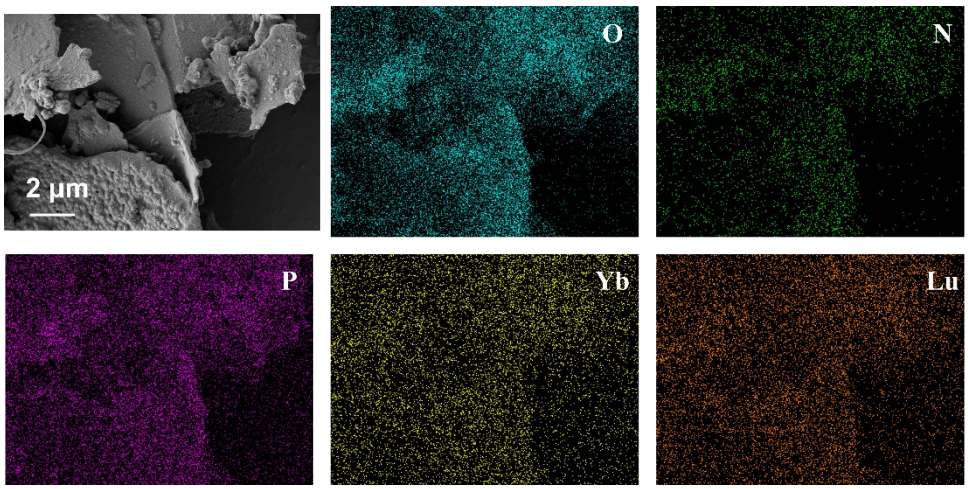

Figure S22 The EDS mapping of M-COF@P507 after adsorption Yb/Lu.

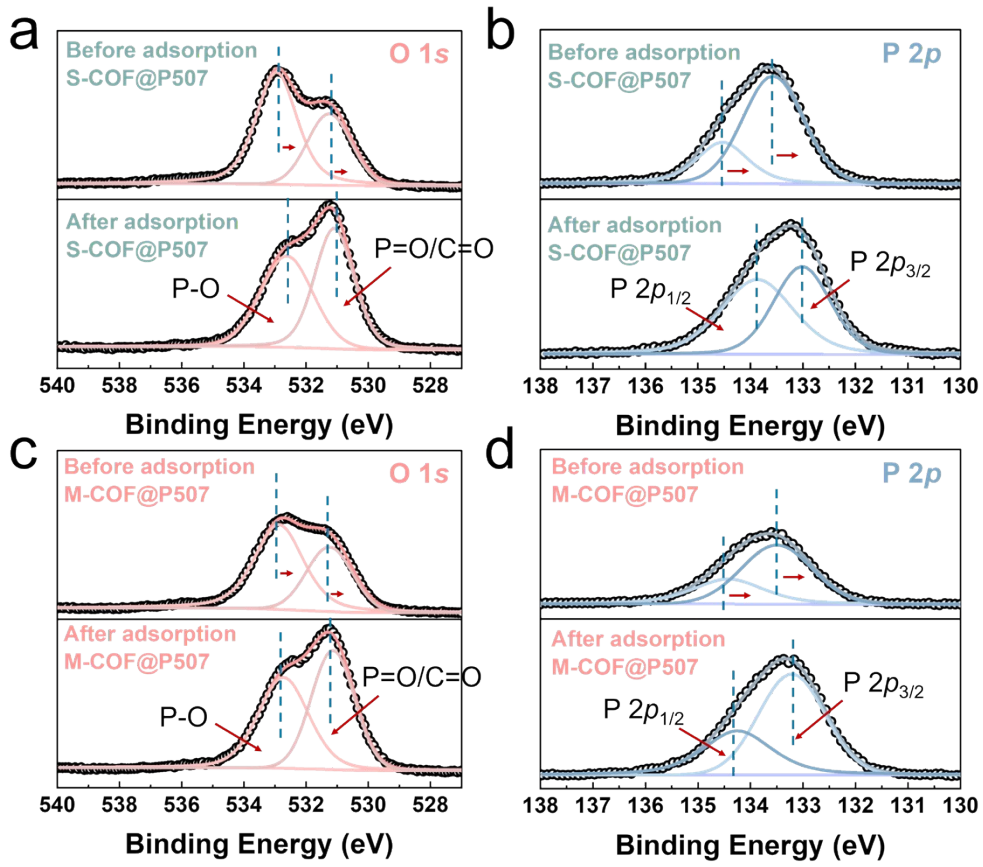

Figure S23 The XPS high resolution spectra of (a), (c) O 1*s*, (b), (d) P 2*p* of S-COF@P507 and M-COF@P507 before and after adsorption Yb/Lu.

Section S5 Theoretical calculation

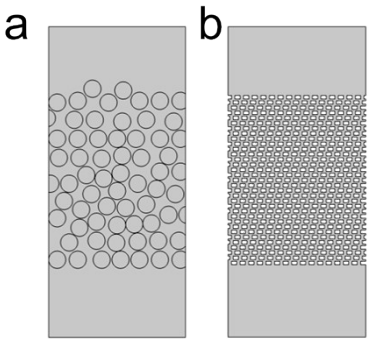

Figure S24 The geometric model of (a) the random spherical model, and (b) the COF membrane model.

The computational domain was discretized using a free triangular mesh, comprising a total of 22,242 elements. The mesh quality was evaluated, showing an average element quality of 0.8244 and a minimum element quality of 0.2043, indicating satisfactory mesh resolution for the simulation. The coupled physics of flow field and dilute species transport were solved simultaneously, governed by the following governing equations:

$$\rho\frac{\partial u}{\partial t} + \rho(u\cdot\nabla)u = \nabla\cdot[-pI + K] + F$$

$$\rho\nabla\cdot u = 0$$

$$\nabla\cdot J_i + u\cdot\nabla c_i = R_i$$

$$J_i = -D_i\nabla c_i$$

Section S6 Column separation

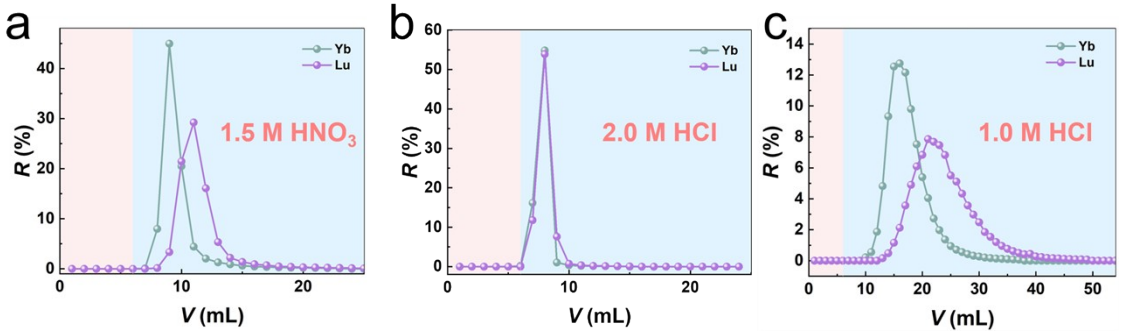

Figure S25 Dynamic elution curve of separation of Yb^{3+}/Lu^{3+} (h = 3.5 cm, *I.D.* = 0.5 cm, light pink and light blue indicates that the eluent is 0.1 M HNO_3 (HCl) and 1.0 M HNO_3 (HCl) solution, respectively): effect of M-COF@P507 column eluting by (a) 1.5 M HNO_3, (b) 2.0 M HNO_3 , and (c) 1.0 M HCl.

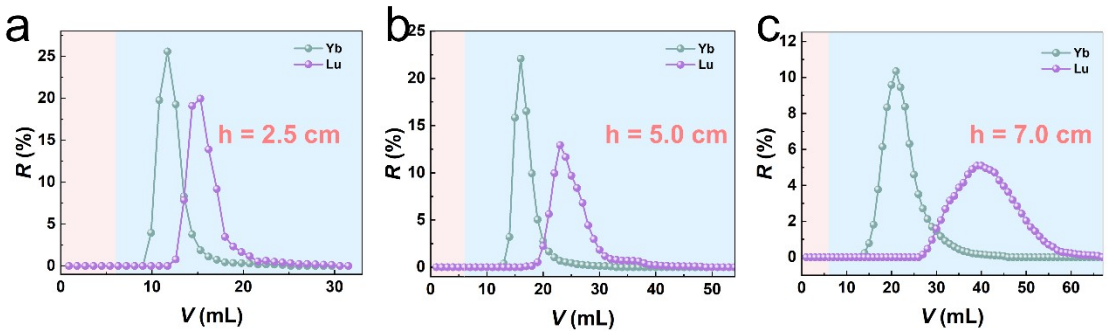

Figure S26 Dynamic elution curve of separation of Yb^{3+}/Lu^{3+} (h = 3.5 cm, *I.D.* = 0.5 cm, light pink and light blue indicates that the eluent is 0.1 M HNO_3 and 1.0 M HNO_3 solution, respectively): effect of M-COF@P507 column height at (a) 2.5, (b) 5.0, and (c) 7.0 cm, respectively.

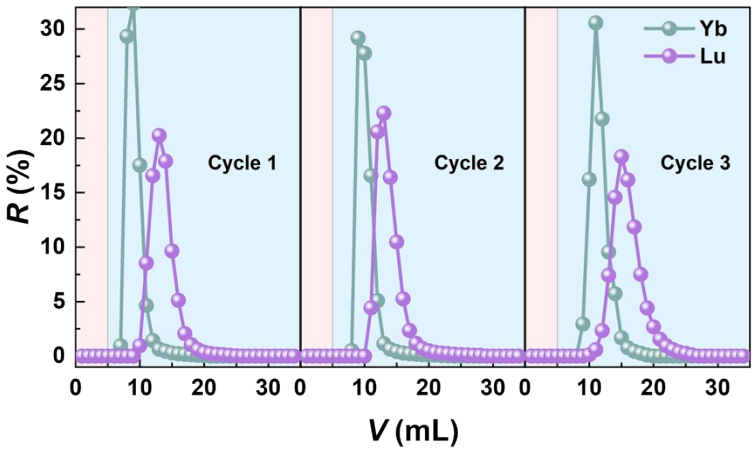

Figure S27 The cyclic dynamic elution curves of Yb^{3+}/Lu^{3+} separation (h = 3.5 cm, *I.D.* = 0.5 cm, light pink and light blue indicate the eluent of 0.1 M HNO_3 and 1.0 M HNO_3 solutions, respectively).

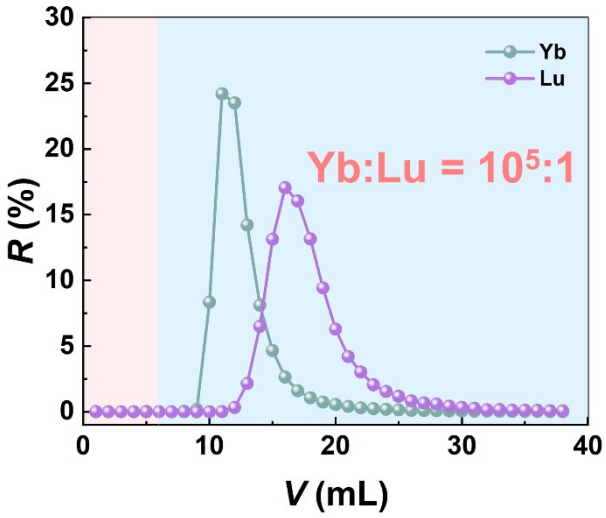

Figure S28 Dynamic elution curve of separation of Yb^{3+}/Lu^{3+} (h = 3.5 cm, *I.D.* = 0.5 cm, light pink and light blue indicates that the eluent is 0.1 M HNO_3 and 1.0 M HNO_3 solution, respectively): effect of simulate target solution Yb^{3+}/Lu^{3+}(^{177}Lu) mass ratio at 10^5:1.

Section S7 Tables

Table S1 The effect of S-COF@P507 and M-COF@P507 packed column separation Yb^{3+}/Lu^{3+} ($m_{Yb} = m_{Lu}$ = 10 μg, *h* = 3.5 cm, *I.D.* = 0.5 cm, C_{HNO3} = 1.0 M, T = 25 ºC).

Materials	m(Lu)/m(Yb)	V (mL)	R_{Lu}(%)	DF
S-COF@P507	1 : 1	27-55	60.4	4.3
M-COF@P507	1 : 1	18-39	87.4	11.9

Table S2 Langmuir and Freundlich parameters for the sorption of Yb^{3+} by S-COF and M-COF.

	Langmuir			Freundlich		
sorbent	q_{max} (mg/g)	b (L/mg)	R^2	K_F (L/g)	n	R^2
S-COF	51.1	0.273	0.9997	37.4	19.3	0.9742
M-COF	50.5	0.476	0.9998	37.7	19.8	0.9938

Table S3 Langmuir and Freundlich parameters for the sorption of Lu^{3+} by S-COF and M-COF.

	Langmuir			Freundlich		
sorbent	q_{max} (mg/g)	b (L/mg)	R^2	K_F (L/g)	n	R^2
S-COF	81.6	0.093	0.9992	46.9	12.9	0.8822
M-COF	83.7	0.064	0.9971	45.9	12.2	0.8646

Table S4 Parameters for kinetic models of Yb^{3+}/Lu^{3+} adsorption by M-COF and S-COF.

Nuclide	Sample	$Q_e^{(exp)}$ (mg/g)	Pseudo-first-order			Pseudo-second-order		
			k_1 (1/h)	$Q_e^{(cal)}$ (mg/g)	R_1^2	k_1 (g/mg/h)	$Q_e^{(cal)}$ (mg/g)	R_2^2
Lu	M-COF	66.0	0.087	38.2	0.817	0.005	69.3	0.995
	S-COF	64.0	0.095	39.2	0.966	0.006	66.1	0.995
Yb	M-COF	48.5	0.067	23.3	0.556	0.005	51.0	0.994
	S-COF	47.5	0.094	31.3	0.711	0.003	52.4	0.992

Table S5 The effect of elution agent for separation Yb^{3+}/Lu^{3+} (m_{Yb} = m_{Lu} = 10 μg, h = 3.5 cm, *I.D.* = 0.5 cm, T = 25 ºC).

m(Lu)/m(Yb)	elution agent	V (mL)	R_{Lu}(%)	DF
1 : 1	1.0 M HNO_3	18-39	87.4	11.9
1 : 1	1.5 M HNO_3	11-26	58.0	6.0
1 : 1	2.0 M HNO_3	9-15	9.2	5.4
1 : 1	1.0 M HCl	20-49	70.4	4.1

Table S6 The effect of column height (h) separation Yb^{3+}/Lu^{3+} (m_{Yb} = m_{Lu} = 10.0 μg, C_{HNO3} = 1.0 M, *I.D.* = 0.5 cm, T = 25 ºC).

m(Lu)/m(Yb)	h (cm)	V (mL)	R_{Lu}(%)	DF
1 : 1	2.5	16-33	74.1	6.4
1 : 1	3.5	18-39	87.4	11.9
1 : 1	5.0	21-48	81.8	14.7
1 : 1	7.0	30-66	85.8	12.5

Table S7 Column parameters of cycling experiments for separation of Yb^{3+}/Lu^{3+} by M-COF@P507 multistage membrane columns (m_{Yb} = m_{Lu} = 10 μg, *h* = 3.5 cm, *I.D.* = 0.5 cm, C_{HNO3} = 1.0 M, T = 25 ºC).

Cycle	m(Lu)/m(Yb)	V (mL)	R_{Lu}(%)	DF
1	1 : 1	10-25	82.7	10.2
2	1 : 1	11-28	81.1	9.5
3	1 : 1	12-28	80	9.0

Table S8 M-COF@P507 column parameters for separating ^{177}Lu (d = 0.5 cm, h = 3.5 cm).

m(Lu)/m(Yb)	elution agent	V (mL)	R_{Lu}(%)	DF
1 : 100000	1.0 M HNO_3	15-36	90.9	7.2

References

1. H. Peng, F. Li, Y. Qin, S. Shi, G. Ma, X. Fan, Y. Li, L. Ma and N. Liu, *ACS Applied Materials & Interfaces*, 2024, **16**, 9343-9354.
2. G. Ma, H. Peng, X. Fan, Y. Li, J. Gao, Y. Hu, B. Li, Y. Yang, J. Zhang, L. Ma, N. Liu, J. Liao and F. Li, *Carbon*, 2024, **225**, 119035.
3. T. Ma, L. Wei, L. Liang, S. Yin, L. Xu, J. Niu, H. Xue, X. Wang, J. Sun, Y.-B. Zhang and W. Wang, *Nature Communications*, 2020, **11**.
4. B. Li, Z. Wang, Z. Gao, J. Suo, M. Xue, Y. Yan, V. Valtchev, S. Qiu and Q. Fang, *Advanced Functional Materials*, 2023, **33**.
5. Y. Chen, Z.-L. Shi, L. Wei, B. Zhou, J. Tan, H.-L. Zhou and Y.-B. Zhang, *Journal of the American Chemical Society*, 2019, **141**, 3298-3303.